Journal of Applied Physics

RESEARCH ARTICLE | JULY 01 2022

Kick-out diffusion of Al in 4H-SiC: an *ab initio* study

Yuanchao Huang ; Yixiao Qian; Yiqiang Zhang; Deren Yang ; Xiaodong Pi

J. Appl. Phys. 132, 015701 (2022)
https://doi.org/10.1063/5.0096577

08 April 2024 02:49:20

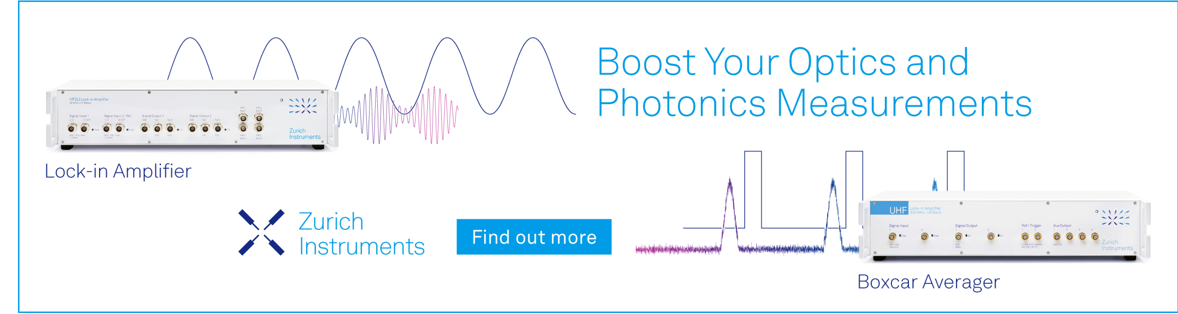

Journal of Applied Physics ARTICLE scitation.org/journal/jap

Kick-out diffusion of Al in 4H-SiC: an *ab initio* study

Cite as: J. Appl. Phys. **132**, 015701 (2022); doi: 10.1063/5.0096577
Submitted: 19 April 2022 · Accepted: 26 May 2022 ·
Published Online: 1 July 2022

View Online

Export Citation

CrossMark

Yuanchao Huang,[1,2] Yixiao Qian,[2] Yiqiang Zhang,[3] Deren Yang,[1,2] and Xiaodong Pi[1,2,a)]

AFFILIATIONS

[1]State Key Laboratory of Silicon Materials & School of Materials Science and Engineering, Zhejiang University, Hangzhou 310027, China
[2]Institute of Advanced Semiconductors & Zhejiang Provincial Key Laboratory of Power Semiconductor Materials and Devices, Hangzhou Innovation Center, Zhejiang University, Hangzhou 311200, China
[3]School of Materials Science and Engineering & College of Chemistry, Zhengzhou University, Zhengzhou, Henan 450001, China

[a)]**Author to whom correspondence should be addressed:** xdpi@zju.edu.cn

ABSTRACT

As a semiconductor with a wide bandgap, 4H silicon carbide (4H-SiC) has considerable potential for high-temperature and high-power devices. It is widely established that *p*-type 4H-SiC is formed predominantly by doping Al. Although Al diffusion in 4H-SiC is often negligible at low temperatures due to the tight bonding of Al in 4H-SiC, the diffusion coefficient of Al dramatically rises when the temperature is rather high. While diffusion is the most fundamental physical processes, the diffusion mechanism of Al in 4H-SiC remains unknown. Due to the large atomic radius of Al relative to the host Si/C atoms and the fact that Al occupies the Si lattice in 4H-SiC, the diffusion of Al is typically mediated by point defects such as vacancies and self-interstitials. We now investigate the diffusion of Al in 4H-SiC using first-principles calculations and compare the activation energy of Al diffusion mediated by carbon vacancies (V_C) to that of Al diffusion mediated by Si interstitials (Si_i). It is found that Al diffusion is actually a Si_i-mediated process, in which a nearby Si_i first kicks a substitutional Al atom to an interstitial site. The kicked-out Al then spreads via interstitial sites. The diffusion coefficient is calculated, which is comparable to experimental results.

Published under an exclusive license by AIP Publishing. https://doi.org/10.1063/5.0096577

08 April 2024 02:49:20

I. INTRODUCTION

A thorough understanding of impurity diffusion is required to tune the properties of semiconductor materials and devices. The diffusion of impurities such as H,[1–3] Li,[4] N,[5] B,[6–9] and Cl[10] has been already studied before for 4H silicon carbide (4H-SiC), which is gaining significant momentum in the development of a number of significant applications such as high-power electronics.[11–13] Al is the most often utilized *p*-type dopant for 4H-SiC because it has lower ionization energy (0.23 eV) than other group-III impurities.[14–21] Due to the strong bonding of Al in 4H-SiC, Al diffusion in 4H-SiC is often insignificant at low temperature. This explains why ion implantation rather than diffusion is used to produce Al-doped regions during the fabrication of 4H-SiC devices.[17,22] However, once high temperature is used, the diffusion of Al in 4H-SiC must be considered. The diffusion coefficient of Al dramatically rises if temperature is rather high. Moreover, it was discovered that after the annealing of Al implanted 4H-SiC, Al laterally straggled in a range from 500 nm to several micrometers at 1200–1800 °C.[23–27] This would have a significant effect on the performance of MOSFETs based on 4H-SiC.

The diffusion coefficient of Al in 4H-SiC is 2×10^{-15} cm^2/s at 1700 °C[28], 3×10^{-14}–6×10^{-12} cm^2/s at temperatures higher than 2500 °C[29] and 2.7×10^{-14} cm^2/s during 1800 °C annealing after ion implantation.[30] It has been reported that the diffusion of Al can be enhanced in 4H-SiC during ion implantation at high temperature.[28,31,32] Usov *et al.*[28] implanted Al into 6H-SiC wafers at 1700 °C, showing the widening of the Al concentration profile in the near-surface region and the anomalous deep penetration tail compared with the Gaussian distribution of the Al profiles of the sample implanted at room temperature. They reported diffusion coefficient in the ranges of 1.5×10^{-12}–2×10^{-14} cm^2/s and 5×10^{-11}–2×10^{-12} cm^2/s in the near- and far-surface regions, respectively. The diffusion coefficients in both regions decreased with increasing

Published under an exclusive license by AIP Publishing

implantation time. Mokhov *et al.* investigated the distribution of implanted Al using second ion mass spectroscopy (SIMS), determining that the activation energy for Al diffusion is about 6.1 eV.[33] By analyzing Vodakov *et al.*'s work on implanted Al, we estimate that the activation energy of the diffusion of Al is about 8.2 eV.[34] However, the Al diffusion behavior is not well understood. The different mechanisms that govern the diffusion process in crystalline solids mainly depend on the type and size of atoms, solubility limit, temperature, and behavior of the dopant atoms in the host lattice. Substitutional, interstitial, and interstitialcy mechanisms are dominant in the case of SiC. H and Li are largely dispersed at the interstitial sites in SiC owing to their small atomic radius, and the diffusion process is interstitial diffusion. The diffusion of N is mediated by mobile carbon $(CC)_C$ split interstitals. When a mobile $(CC)_C$ split interstitial approaches a substitutional N at a C lattice, $(NC)_C$ split interstitials are formed. $(NC)_C$ split interstitials may travel across the lattice after they have been generated. The diffusion of substitutional B at a Si lattice site is achieved by a neighboring Si interstitial kicking out the substitutional B into the interstitial sites. Cl diffuses through SiC by a vacancy-mediated process.[10] Due to the large atomic radius of Al relative to the host Si/C atoms and the fact that Al occupies the Si lattice in silicon carbide, the diffusion of Al may be mediated by points defects, which may be either vacancies or interstitials. Up to know, however, the exact mechanism for the diffusion of Al in 4H-SiC has not been clarified.

First-principles calculations may aid in the direct investigation of diffusion processes from a microscopic and atomistic perspective, and particular quantitative diffusion coefficients.[35–38] In light of this, this paper employs first-principles calculations to investigate the Al diffusion process in 4H-SiC. The mechanisms of vacancy-mediated diffusion and interstitial-mediated diffusion (kick-out diffusion) are discussed. The activation energy of the two diffusion processes is compared. It is determined that Al diffusion follows the kick-out diffusion mechanism. Finally, the diffusion coefficient of Al is estimated.

II. COMPUTATIONAL METHODS

A. First-principles calculations

First-principles calculations are performed using the projector-augmented wave (PAW) method implanted in the Vienna *ab-initio* Simulation Package (VASP).[39] The wave functions are expanded by using the plane wave energy cutoff of 500 eV. The Perdew–Burke–Ernzerhof (PBE) functional with a generalized gradient approximation (GGA) exchange-correlation is employed to describe the exchange-correlation interactions. Brillouin-zone integrations are approximated by using special k-point sampling of the Monkhorst–Pack scheme with a k-point mesh of $2 \times 2 \times 2$. The supercell lattice and atomic coordinates are fully relaxed until the total energy per cell and the force on each atom are less than 1.0×10^{-6} eV and 0.01 eV/Å, respectively. The screened hybrid density functional of Heyd, Scuseria, and Ernzerhof (HSE06) is adopted to calculate the electronic properties of 4H-SiC. Defects are modeled in a $6 \times 6 \times 2$ supercell of 4H-SiC with 576 atoms. The calculated lattice parameters of 4H-SiC are $a = 3.07$ Å and $c = 10.05$ Å. The calculated bandgap energy of 4H-SiC is 3.18 eV, which agrees well with experimental results.[1]

B. Defect-formation calculations

The formation energy of a defect α at the charge state q in 4H-SiC is calculated by using[40–42]

$$\Delta H_f(\alpha, q) = \Delta E(\alpha, q) + \sum n_i \mu_i + qE_F, \tag{1}$$

where $\Delta E(\alpha, q) = E(\alpha, q) - E(\mathrm{SiC}) + \sum n_i E(i) + q\varepsilon_{\mathrm{VBM}}$, where $E(\alpha, q)$ is the total energy of the SiC supercell containing defect α at charge state q; $E(\mathrm{SiC})$ is the total energy of the SiC supercell; E_F is the Fermi energy referred to the VBM (E_V) of SiC; n_i is the number of atoms removed from or added into the supercell; and μ_i is the chemical potential of constituent, where i is referred to elemental solid or gas with energy $E(i)$.

Thermal-equilibrium conditions exert a series of thermodynamic limits on the achievable values of μ_i. First, the values of μ_i are limited to those values that maintain a stable SiC,

$$\mu_{\mathrm{Si}} + \mu_{\mathrm{C}} = \Delta H_f(\mathrm{SiC}). \tag{2}$$

Second, for the avoidance of the precipitation of Si, C, and Al, the values of μ_i are limited by

$$\mu_{\mathrm{Si}} \le 0,\ \mu_{\mathrm{C}} \le 0,\ \ \mu_{\mathrm{Al}} \le 0. \tag{3}$$

Finally, for the avoidance of the formation of secondary phases of Al_4C_3, the values of μ_i are limited by

$$4\mu_{\mathrm{Al}} + 3\mu_{\mathrm{C}} \le \Delta H_f(\mathrm{Al_4C_3}), \tag{4}$$

where $\Delta H_f(\mathrm{Al_4C_3})$ is the formation energy of Al_4C_3.

C. Migration barrier calculations

The migration energy of Al in 4H-SiC is investigated by using Climbing Image Nudge Elastic Band (CI-NEB) with $2 \times 2 \times 2$ k-point mesh. The CI-NEB method is an effective method for finding the saddle points and minimum energy paths between the initial and final states.[43] The total energy and force on each atom are converged to $< 1.0 \times 10^{-6}$ eV and < 0.0001 eV/Å, respectively. The number of images depends on the distance of the diffusion path between the initial and final states, which ensures that the distance between each image is not less than 0.8 Å.

In general, diffusion coefficient in the basal plane is different from that out of plane. For simplicity, we approximate the diffusion as isotropic. This approximation is reasonable because we find that in-plane and out-of-plane migration paths for the diffusion dominating species are comparable. The difference between the in-plane jump distance and out-of-plane jump distance (3.02 Å) has a small effect compared to the order of magnitude of the variations in the diffusion coefficient. The diffusion coefficient is calculated by using

$$D = D_0 \exp\left(-\frac{E_a}{kT}\right), \frac{z}{6} \nu a^2 \exp\left(-\frac{E_a}{kT}\right), \tag{5}$$

where D_0 is the diffusion prefactor, E_a is the activation energy, z/6 is a geometric factor, α is the jump distance in the basal plane,

08 April 2024 02:49:20

Published under an exclusive license by AIP Publishing

and ν is the attempt frequency calculated with

$$\nu = \prod_{i=1}^{3N-3} \omega_i / \prod_{j=1}^{3N-4} \omega_j \tag{6}$$

where ω_i denotes the vibrational frequency of the initial state and ω_j for the transition state. The vibrational frequencies are calculated by using the finite displacement approach. We finally obtain that D_0 is about 4.3×10^4 cm^2/s.

III. RESULTS AND DISCUSSIONS

The diffusion mediated by carbon vacancy (V_C) is explored in this study. There are two major causes for this. First, V_C has a substantially lower formation energy than that of the other intrinsic defects. Our earlier research demonstrated that when Al doping concentration increases, Fermi energy advances toward the valence band for *p*-type SiC. The formation energy of V_C may be greatly decreased to compensate for *p*-type doping. Second, Gali *et al.* demonstrated that V_C could bind to Al_{Si}, forming extremely stable $Al_{Si} + V_C$ complexes.[44]

Figures 1(a) and 1(b) show the calculated defect formation energies of Al_{Si}, V_C, and $Al_{Si} + V_C$ in 4H-SiC at the Si-rich and C-rich limits. Generally, Al is energy favorable located at the Si sublattice than when it is located at the C sublattice. The formation energies of Al_{Si} at the quasihexagonal (h) and quasicubic (k) sites of Si are similar. The calculated (0/−) transition energy of Al_{Si} is $E_V + 0.23$ eV, which is consistent with the experimental data.[1] For V_C, negative-U behavior is found at both k and h sites. The (0/−2) transition energy levels are $E_V + 2.60$ and $E_V + 2.67$ eV for V_C(k) and V_C(h), respectively. The (2+/0) transition levels of V_C(h) and V_C(k) are located at $E_V + 1.84$ and $E_V + 1.90$ eV, respectively. This is well agreed with electron paramagnetic resonance (EPR) and deep-level transient spectroscopy (DLTS) measured results.[45–47] For $Al_{Si} + V_C$, when the Fermi energy changes from E_V to $E_V + 2.61$ eV, $Al_{Si} + V_C$ is in a 1+ charge state. When the Fermi energy changes from $E_V + 2.61$ to $E_C + 3.20$ eV, $Al_{Si} + V_C$ is in 3− charge. The binding energy of the $Al_{Si} + V_C$ complex $[E_b(Al_{Si} + V_C)]$ is calculated by $E_b(Al_{Si} + V_C) = \Delta H_f(Al_{Si}) + \Delta H_f(V_C) - \Delta H_f(Al_{Si} + V_C)$. As shown in Fig. 1(c), $E_b(Al_{Si} + V_C)$ for *p*-type 4H-SiC is positive, indicating that the $Al_{Si} + V_C$ complex is stable against decomposition into individual Al_{Si} and V_C interstitials.

Figures 1(d) and 1(e) show the atomic model and calculated migration barrier of $Al_{Si} + V_C$ in the 1+ and 3− charge states. With the assistance of V_C, the diffusion of Al_{Si} is achieved through directly exchanging the closest neighbor Si, as shown in Fig. 1(d). The calculated migration barriers are both about 14.4 eV for the 1+ and 3− charge states.

For B diffusion in SiC, the "kick-out mechanism" is well known.[9–12] That is, a neighboring interstitial Si kicks the substitutional B at a Si lattice site out to an interstitial site, following which, B diffuses out at interstitial sites. Is Al diffusion in the same way? A Si_i must be near to an Al_{Si} in order for kick-out diffusion to occur. For Si_i, four types of interstitial sites are considered. Si_i^{C-te} and Si_i^{Si-te} are the Si atoms located at the carbon and silicon coordinated tetrahedral sites, respectively. Si_i^{Si-C} is the Si atom located at the

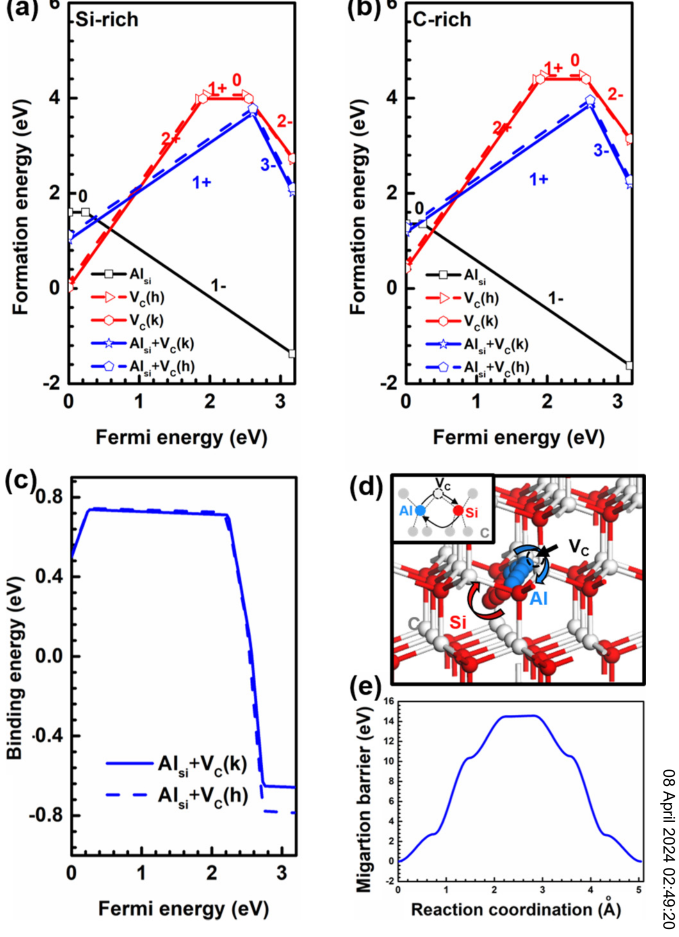

FIG. 1 (a) Calculated defect formation energies of Al_{Si}, V_C and Al_{Si}+V_C in 4H-SiC at the Si-rich limit. (b)Calculated defect formation energies of Al_{Si}, V_C and Al_{Si}+V_C in 4H-SiC at the C-rich limit. (c) Calculated binding energy of the Al_{Si}+V_C complex in 4H-SiC. (d) Atomic configurations of Al_{Si} with the assistance of V_C. (e) Calculated migration barriers of Al_{Si} with the assistance of V_C.

hexagonal layer accommodating an equal carbon- and silicon-coordinated site. Si_i^{hex} is the Al atom located at the site encompassed by the upper and lower hexagonal basal planes. Si_i^{Si-te} is thermodynamically unstable, and it cannot be obtained through DFT structural relaxation. As shown in Figs. 2(a) and 2(b), among Si_i^{C-te}, Si_i^{Si-C}, and Si_i^{hex}, Si_i^{C-te} has the lowest formation energy and is in 4+ charge state for *p*-type 4H-SiC (Fermi energy closed to E_V). Figures 2(a) and 2(b) also show the formation energies of $Al_{Si} + Si_i^{C-Si}$, $Al_{Si} + Si_i^{C-te}$, and $Al_{Si} + Si_i^{hex}$. Throughout the Fermi energy, $Al_{Si} + Si_i^{C-te}$ and $Al_{Si} + Si_i^{hex}$ have the lowest formation energies. At the Si-rich limit, when the Fermi energy increases from E_V to $E_V + 2.0$ eV, the formation energy of $Al_{Si} + Si_i^{C-te}$ in the 3+ charge state is the lowest, increasing from 1.6 to 7.6 eV. When the Fermi energy is greater than $E_V + 2.0$ eV, the formation energy of $Al_{Si} + Si_i^{hex}$ in the 1− charge state is the lowest (8.0 eV).

08 April 2024 02:49:20

Published under an exclusive license by AIP Publishing

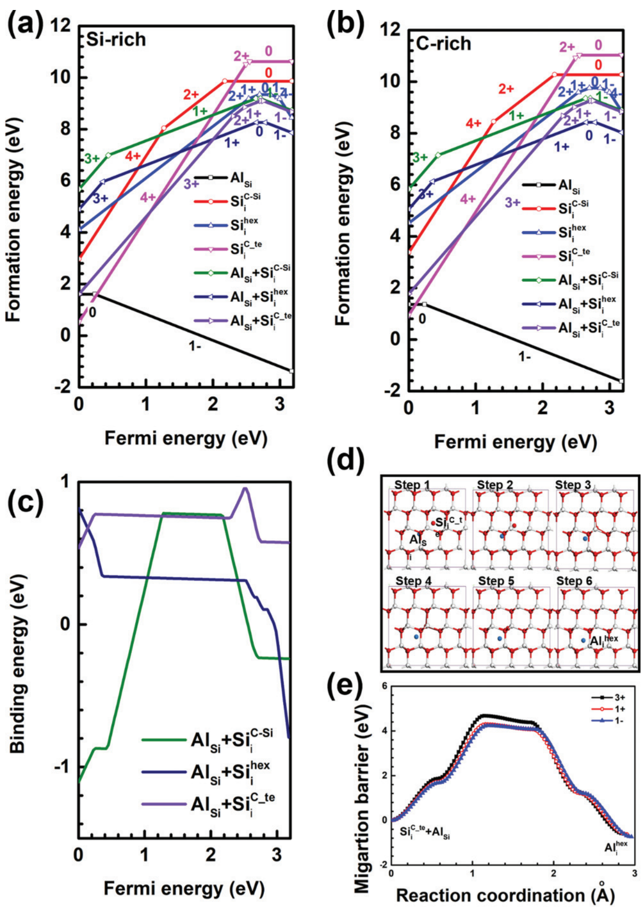

FIG. 2 (a) Calculated defect formation energies of Al_{Si}, interstitial Si_i and Al_{Si}+Si_i in 4H-SiC at the Si-rich limit. (b) Calculated defect formation energies of Al_{Si}, interstitial Si and Al_{Si}+Si_i in 4H-SiC at the C-rich limit. (c) Calculated binding energy of the Al_{Si}+Si_i complex in 4H-SiC. (d) Atomic configurations of the kick-out of Al. (e) Calculated migration barriers of the kick-out of Al.

Furthermore, the binding energies of $Al_{Si} + Si_i^{C-Si}$, $Al_{Si} + Si_i^{C-te}$, and $Al_{Si} + Si_i^{hex}$ are estimated [Fig. 2(c)]. It shows that the binding energies of $Al_{Si} + Si_i^{C-te}$ and $Al_{Si} + Si_i^{hex}$ are positive, indicating that Si_i^{C-te} and Si_i^{hex} are both energetically favorable to attach with Al_{Si}.

Si interstitially advances toward the substitutional Al and kicks it into the interstitial site during the kick-out process, which corresponds to the change from $Al_{Si} + Si_i$ to Al_i ($Al_{Si} + Si_i \leftrightarrow Al_i$). There are total six fundamental processes considered, $Si_i^{C-Si} + Al_{Si} \rightarrow Al_i^{C_te}$, $Si_i^{C-Si} + Al_{Si} \rightarrow Al_i^{Si_te}$, $Si_i^{hex} + Al_{Si} \rightarrow Al_i^{C_te}$, $Si_i^{hex} + Al_{Si} \rightarrow Al_i^{Si_te}$, $Si_i^{C_te} + Al_{Si} \rightarrow Al_i^{hex}$, and $Si_i^{C_te} + Al_{Si} \rightarrow Al_i^{C-Si}$. The associated kick-out energy barriers are calculated and summarized in Table I. For example, the energy barrier of $Si_i^{C_te} + Al_{Si} \rightarrow Al_i^{hex}$ is lower than that of $Si_i^{C_te} + Al_{Si} \rightarrow Al_i^{C-Si}$, implying that $Si_i^{C_te}$ would kick Al_{Si} to the hexagonal sites of the next layers. The specific process of the kick-out of $Si_i^{C_te} + Al_{Si} \rightarrow Al_i^{hex}$ is shown in Figs. 2(d) and 2(e). Similarly, $Si_i^{C-Si} + Al_{Si} \rightarrow Al_i^{C_te}$ or $Si_i^{hex} + Al_{Si} \rightarrow Al_i^{C_te}$ is more likely to occur if Si_i^{C-Si} or Si_i^{hex} is close to Al_{Si}. After Al_{Si} is kicked out and forms Al_i, Al_i can diffuse out along the interstitial sites. In the (0001) plane, there are two types of diffusion. One is $Al_i^{C_te} \rightarrow Al_i^{Si_te} \rightarrow Al_i^{C_te}$ with a migration barrier of about 2.4 eV. The other is $Al_i^{hex} \rightarrow Al_i^{C-Si} \rightarrow Al_i^{hex}$ with a migration barrier of about 2.6 eV. Out-of-plane migration paths are mainly $Al_i^{C_te}$, $Al_i^{Si_te}$, Al_i^{hex}, and Al_i^{C-Si} moving to the Si lattice site and forming a splitting interstitial Al_i^{Split}. The migration barrier is about 2.6–2.8 eV. In-plane and out-of-plane migration barriers are similar. Furthermore, since the energy needed for Al_i diffusion is much smaller than that required for kick-out, the kick-out process is the limiting step.

TABLE I. The kick out/in energy barriers of Al with Si_i.

Kick-out mechanism	Kick-out (eV)	Kick-in (eV)
$Si_i^{C-Si} + Al_{Si} \rightarrow Al_i^{C_te}$	+3 : 3.698 419	+3 : 7.376 919
	+1 : 5.610 646	+1 : 6.391 177
	−1 : 5.512 021	−1 : 6.292 552
$Si_i^{C-Si} + Al_{Si} \rightarrow Al_i^{Si_te}$	+3 : 4.194 334	+3 : 7.342 454
	+1 : 5.965 642	+1 : 6.791 234
	−1 : 5.713 490	−1 : 6.519 783 1
$Si_i^{hex} + Al_{Si} \rightarrow Al_i^{C_te}$	+3 : 4.677 863	+3 : 5.272 699
	+1 : 4.295 279	+1 : 4.917 689
	−1 : 4.240 353	−1 : 4.975 843
$Si_i^{hex} + Al_{Si} \rightarrow Al_i^{Si_te}$	+3 : 4.819 304	+3 : 5.572 435
	+1 : 4.635 170	+1 : 5.256 209
	−1 : 4.701 254	−1 : 5.343 401
$Si_i^{C_te} + Al_{Si} \rightarrow Al_i^{hex}$	+3 : 3.810 759	+3 : 6.135 063
	+1 : 4.403 963	+1 : 4.699 412
	−1 : 4.442 973	−1 : 4.529 2
$Si_i^{C_te} + Al_{Si} \rightarrow Al_i^{C-Si}$	+3 : 3.910 278	+3 : 6.214 253
	+1 : 4.780 012	+1 : 4.901 456
	−1 : 4.641 290	−1 : 4.854 512

The activation energy of a diffusion process is the sum of the formation energy and the migration barrier. It turns out that the Si-rich and C-rich cases hardly affect the activation energy, as demonstrated in Fig. 3(a) and (b). The activation energy of V_C-mediated Al diffusion is greater than that of kick-out diffusion throughout the entire Fermi energy range. As a result, the kick-out diffusion process is definitely the major mechanism for Al diffusion. When the Fermi energy changes from E_V to $E_V + 1.4\,e_V$, $Si_i^{C_te}$ kick-out Al diffusion is dominant with the activation energy increasing from 7.7 to 11.9 eV. When the Fermi energy changes from $E_V + 1.4$ eV to $E_V + 3.18$ eV, Si_i^{hex} kick-out Al diffusion is dominant with the activation energy rising to around 13 eV. The activation energy of Al diffusion in an Al heavy doped 4H-SiC may be estimated to be about 7.7 eV, which is 1.6 eV higher than Mokhov's findings and 0.5 eV lower than Vodakov's, which is acceptable when the experimental error and computational error are taken into account. Moreover, the diffusion coefficient of Al in 4H-SiC is calculated according to

08 April 2024 02:49:20

Published under an exclusive license by AIP Publishing

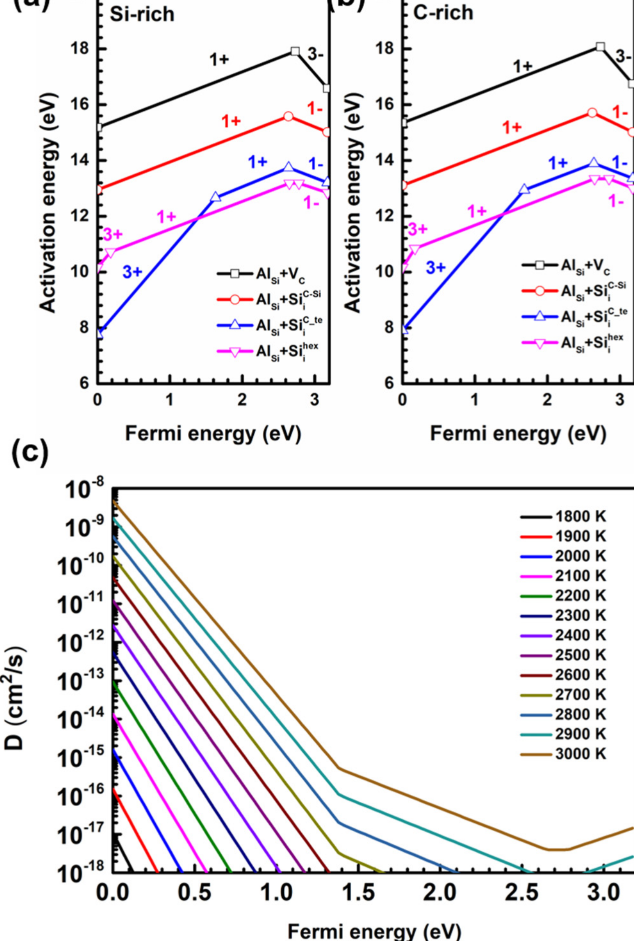

FIG. 3. (a) Activation energy of V_C or interstitial-mediated Al diffusion at the Si-rich limit. (b) Activation energy of V_C or interstitial-mediated Al diffusion at the C-rich limit. (c) The calculated diffusion coefficients of Al in 4H-SiC at various temperatures.

Eq. (5), as shown in Fig. 3(c). The diffusion coefficient of Al in *p*-type SiC is larger than that in *n*-type SiC. The diffusion coefficient decreases as the Fermi level approaches the conduction band. At temperature below 1800 K, the diffusion coefficient is less than 10^{-17} cm^{-3}. When the temperature is elevated to 2400 K, the diffusion coefficient may increase to 10^{-12} cm^{-3}.

IV. CONCLUSION

In conclusion, we have investigated the diffusion mechanism of Al in 4H-SiC by using first-principles calculations. It is found that Al diffuses in 4H-SiC through a kick-out process, in which an adjacent Si interstitial first kicks substitutional Al to the interstitial sites. The resulting interstitial Al then diffuses along the interstitial sites. The activation energy of Al diffusion varies with the Fermi energy. The lowest activation energy is 7.7 eV. We have also calculated the diffusion coefficient of Al in 4H-SiC, which may be impacted by the Fermi energy and temperature.

ACKNOWLEDGMENTS

This work is supported by “Pioneer” and “Leading Goose” R&D Program of Zhejiang (Grant No. 2022C01021) and the Natural Science Foundation of China (Grant Nos. 91964107 and U20A20209). Partial support from the Natural Science Foundation of China for Innovative Research Groups (Grant No. 61721005) is acknowledged. National Supercomputer Center in Tianjin is thanked for computational support.

AUTHOR DECLARATIONS

Conflict of Interest

The authors have no conflicts to disclose.

Author Contributions

Yuanchao Huang: Conceptualization (equal); Data curation (equal); Formal analysis (equal); Investigation (equal); Methodology (equal). **Yixiao Qian:** Data curation (equal); Methodology (equal). **Yiqiang Zhang:** Supervision (equal). **Deren Yang:** Project administration (equal); Supervision (equal). **Xiaodong Pi:** Funding acquisition (equal); Methodology (equal); Supervision (equal); Writing – original draft (equal).

DATA AVAILABILITY

The data that support the findings of this study are available within the article.

08 April 2024 02:49:20

REFERENCES

[1]M. S. Janson, A. Hallén, M. K. Linnarsson, and B. G. Svensson, Phys. Rev. B **64**, 195202 (2001).
[2]W. Wang, C. Li, S. L. Shang, J. Cao, Z. K. Liu, Y. Wang, and C. Fang, Prog. Nucl. Energy **119**, 103181 (2020).
[3]B. Aradi, P. Deak, A. Gali, N. T. Son, and E. Janzen, Phys. Rev. B **69**, 233202 (2004).
[4]M. K. Linnarsson, M. S. Janson, S. Karlsson, A. Schöner, N. Nordell, and B. G. Svensson, Mater. Sci. Eng. B **61**, 275 (1999).
[5]U. Gerstmann, E. Rauls, T. Frauenheim, and H. Overhof, Phys. Rev. B **67**, 205202 (2003).
[6]Y. Gao, S. I. Soloviev, and T. S. Sudarshan, Appl. Phys. Lett. **83**, 905 (2003).
[7]R. Rurali, P. Godignon, and J. Rebollo, Appl. Phys. Lett. **81**, 2989 (2002).
[8]M. Bockstedte, A. Mattausch, and O. Pankratov, Phys. Rev. B **70**, 115203 (2004).
[9]R. Rurali, E. Hernandez, P. Godignon, J. Rebollo, and P. Ordejon, Phys. Rev. B **69**, 125203 (2004).
[10]G. Alfieri and T. Kimoto, J. Appl. Phys. **113**, 133706 (2013).
[11]T. Kimoto and J. A. Cooper, *Fundamentals of Silicon Carbide Technology: Growth, Characterization, Devices and Applications* (John Wiley & Sons, 2014).
[12]F. F. Wang and Z. Zhang, CPSS Trans. Power Electron. Appl. **1**, 13 (2016).
[13]F. Roccaforte, P. Fiorenza, G. Greco, R. Lo Nigro, F. Giannazzo, F. Iucolano, and M. Saggio, Microelectron. Eng. **187**, 66 (2018).
[14]Y. C. Huang, R. Wang, Y. X. Qian, Y. Q. Zhang, D. Yang, and X. D. Pi, Chin. Phys. B **31**, 046104 (2022).
[15]C. Darmody and N. Goldsman, J. Appl. Phys. **126**, 145701 (2019).

Published under an exclusive license by AIP Publishing

[16]T. Hayashi, K. Asano, J. Suda, and T. Kimoto, J. Appl. Phys. **112**, 064503 (2012).
[17]F. Roccaforte, P. Fiorenza, M. Vivona, G. Greco, and F. Giannazzo, Materials **14**, 3923 (2021).
[18]A. Parisini and R. Nipoti, J. Appl. Phys. **114**, 243703 (2013).
[19]K. Murata, T. Tawara, A. Yang, R. Takanashi, and H. Tsuchida, J. Appl. Phys. **129**, 025702 (2021).
[20]I. D. Booker, H. Abdalla, J. Hassan, R. Karhu, L. Lilja, E. Janzén, and E. Ö. Sveinbjörnsson, Phys. Rev. Appl. **6**, 014010 (2016).
[21]B. Chen, J. Chen, Y. Yao, T. Sekiguchi, H. Matsuhata, and H. Okumura, Appl. Phys. Lett. **105**, 042104 (2014).
[22]V. Heera, D. Panknin, and W. Skorupa, Appl. Surf. Sci. **184**, 307 (2001).
[23]J. Müting, V. Bobal, T. Neset Sky, L. Vines, and U. Grossner, Appl. Phys. Lett. **116**, 012101 (2020).
[24]K. Mochizuki and N. Yokoyama, IEEE Trans. Electron Devices **58**, 455–459 (2011).
[25]E. Morvan, N. Mestres, J. Pascual, D. Flores, M. Vellvehi, and J. Rebollo, Mater. Sci. Eng. B **61–62**, 373–377 (1999).
[26]T. B. Hook, J. Brown, P. Cottrell, E. Adler, D. Hoyniak, J. Johnson, and R. Mann, IEEE Trans. Electron Devices **50**, 1946–1951 (2003).
[27]G. Lulli, IEEE Trans. Electron Devices **58**, 190–194 (2011).
[28]I. O. Usov, A. A. Suvorova, V. V. Sokolov, Y. A. Kudryavtsev, and A. V. Suvorov, J. Appl. Phys. **86**, 6039 (1999).
[29]C. M. Zetterling, *Process Technology for Silicon Carbide Devices* (IET, 2002).
[30]Y. Tajima, K. Kijima, and W. D. Kingery, J. Chem. Phys. **77**, 2592 (1982).
[31]A. V. Suvorov, I. O. Usov, V. V. Sokolov, and A. A. Suvorova, in *Materials Research Society Symposium Proceedings* (MRS, 1996), Vol. 396, p. 239.
[32]I. O. Usov, A. A. Suvorova, V. V. Sokolov, Y. A. Kudryavtsev, and A. V. Suvorov, in *Materials Research Society Symposium Proceedings* (MRS, 1998), Vol. 504, p. 141.
[33]E. N. Mokhov, Sov. Phys. Solid State **11**, 415 (1969).
[34]Y. A. Vodakov and E. N. Mokhof, Silicon Carbide **1974**, 508 (1973).
[35]G. Y. Huang, C. Y. Wang, and J. T. Wang, Scr. Mater. **61**, 324–326 (2009).
[36]A. Höglund, C. W. M. Castleton, and S. Mirbt, Phys. Rev. B **77**, 113201 (2008).
[37]J. Zhu, T. D. dela Rubia, L. H. Yang, C. Mailhiot, and G. H. Gilmer, Phys. Rev. B **54**, 4741 (1996).
[38]J. W. Jeong and A. Oshiyama, Phys. Rev. B **64**, 235204 (2001).
[39]G. Kresse and J. Hafner, Phys. Rev. B **47**, 558 (1993).
[40]S. H. Wei, Comput. Mater. Sci. **30**, 337 (2004).
[41]R. Wang, X. Tong, J. Xu, S. Zhang, P. Zheng, F. X. Chen, and W. Tan, Phys. Rev. Appl. **11**, 054021 (2019).
[42]X. Yan, P. Li, L. Kang, S. H. Wei, and B. Huang, J. Appl. Phys. **127**, 085702 (2020).
[43]G. Henkelman, B. P. Uberuaga, and H. Jónsson, J. Chem. Phys. **113**, 9901 (2000).
[44]A. Gali, T. Hornos, N. T. Son, E. Janzén, and W. J. Choyke, Phys. Rev. B **75**, 045211 (2007).
[45]N. T. Son, X. T. Trinh, L. S. Løvlie, B. G. Svensson, K. Kawahara, J. Suda, and E. Janzén, Phys. Rev. Lett. **109**, 187603 (2012).
[46]K. Kawahara, X. Thang Trinh, N. Tien Son, E. Janzén, J. Suda, and T. Kimoto, Appl. Phys. Lett. **102**, 112106 (2013).
[47]X. T. Trinh, K. Szász, T. Hornos, K. Kawahara, J. Suda, T. Kimoto, A. Gali, E. Janzén, and N. T. Son, Phys. Rev. B **88**, 235209 (2013).

08 April 2024 02:49:20

Published under an exclusive license by AIP Publishing